Band structure effects in interband tunnel devices

D. Z.-Y. Ting, E. T. Yu, and T. C. McGill
Thomas J. Watson, Sr., Laboratory of Applied Physics, California Institute of Technology, Pasadena, California 91125

(Received 29 January 1991; accepted 8 April 1991)

We report on a calculation of transport in InAs/GaSb/AlSb-based interband tunnel structures using a realistic band structure model. The results are compared with calculations using a two-band model which includes only the lowest conduction band and the light-hole band. We find that for device structures containing GaSb quantum wells, the inclusion of heavy-hole states can introduce additional transmission resonances and substantial hole-mixing effects. These effects are found to have a significant influence on the current–voltage characteristics of interband devices.

I. INTRODUCTION

The nearly lattice-matched InAs/GaSb/AlSb material system has received considerable attention recently due to the tremendous flexibility it offers for heterostructure design. As seen in Fig. 1, where the conduction and valence band edges for InAs, GaSb, and AlSb are plotted according to the currently accepted band offset values,[1-3] this material system offers the possibility for type I (GaSb–AlSb), type II staggered (AlSb–InAs), and type II broken-gap (InAs–GaSb) band alignments. Recently, several novel devices which exploit the type II broken-gap band alignment between InAs and GaSb have been demonstrated.[4-11] These devices have been called interband devices since their operation involves both the InAs conduction-band states and the GaSb valence-band states. Various interband devices have exhibited very high peak current densities or large peak-to-valley current ratios, making them extremely attractive for use in high-frequency oscillators, logic circuits, and a variety of other digital and analog applications. For example, a peak-to-valley current ratio of 20 (88) at 300 K (77 K) has been reported in an InAs–AlSb–GaSb–AlSb–InAs device,[4] and negative differential resistance (NDR) with a peak current density of 1.6×10^5 A/cm^2 has been observed in an InAs–GaSb–AlSb–GaSb device.[10] In addition, GaSb–InAs–AlSb–GaSb Stark effect tunneling transistors utilizing interband transport properties have demonstrated high gains at room temperature.[11]

To date, theoretical studies of interband tunneling devices have used simple two-band models which have included only the interaction between the conduction and light-hole bands, and have assumed that interactions involving the heavy-hole and split-off bands are negligible.[12,13] Although this simple approach has been fairly successful in explaining qualitative features observed experimentally,[14] it is somewhat unsatisfactory due to the oversimplification of the valence band structure. In this paper we examine transport in interband devices using a realistic band structure model which correctly treats the coupling among the heavy-hole, light-hole, and split-off valence bands, the coupling of the valence bands to the lowest conduction band, and the spin-orbit interaction. We calculate transmission coefficients and current–voltage (J–V) characteristics for several prototypical interband devices, and compare the results to two-band model calculations.

II. METHODS

Our computation of current–voltage (J–V) characteristics can be divided into three steps. First, band bending corresponding to the given doping profile and applied bias is computed by solving Poisson's equation across the entire device and requiring overall charge neutrality in the structure. Thomas–Fermi screening theory is used to relate the local carrier concentration to the band edge position. Next, transmission coefficients are calculated for device profiles obtained from the band bending calculation. The complexity of this computation depends on the band structure model used to describe the materials in the heterostructure; we will discuss this further below. Finally, the current is computed by including appropriate Fermi factors and velocities, and integrating over the incoming electron distribution[15]:

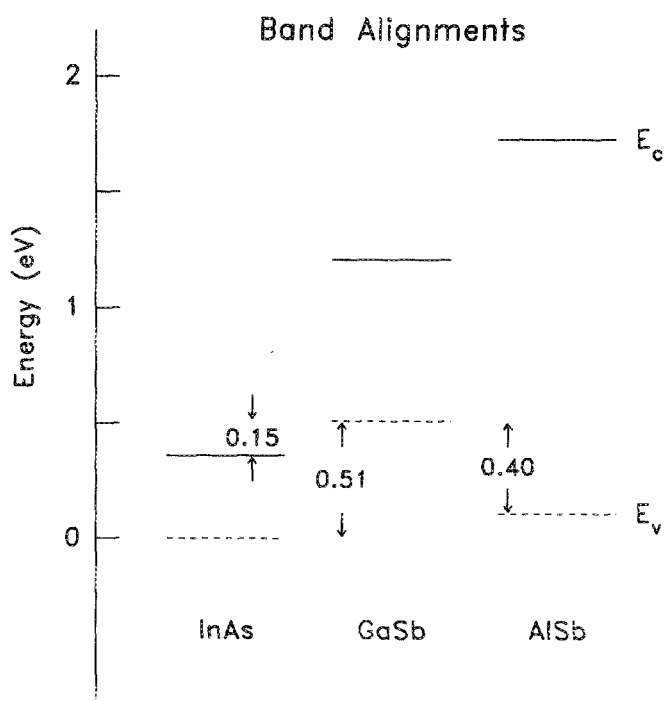

FIG. 1. Conduction (solid) and valence (dashed) band edges for the InAs/GaSb/AlSb material system. The energy gaps and band offsets allow the possibility of type I, type II, and type II broken-gap band alignments. The indirect conduction-band minimum is shown for AlSb.

 0734-211X/91/042405-06$01.00

$$J=\frac{e}{4\pi^3\hbar}\int d^2k_{\parallel}\int dE\,[f(E)-f(E+eV)]\,T(E,\mathbf{k}_{\parallel}). \tag{1}$$

Our calculation stays within the framework of the single-electron picture, and does not include effects due to inelastic scattering. The aim of this calculation is to treat band structure effects accurately to study the influence of the heavy-hole bands.

To include band structure effects properly, we use the eight-band effective bond orbital model,[16] which takes into account the heavy-hole, light-hole, and split-off valence bands and the lowest conduction band. This model, a reformulation of Kane's eight-band **k·p** model[17] in the tight-binding framework, provides a realistic description of the relevant band structure needed for treating interband tunnel devices, and takes advantage of the flexibility of the tight-binding method without requiring any parameter fitting. In treating interband transport with the effective bond orbital model, care must be taken in computing the transmission coefficients. For simple two-band models, transmission coefficients can be obtained using the standard transfer matrix method.[18,19] However, it is well known that the transfer matrix method, when used in conjunction with realistic multiband band structure models, is numerically unstable for devices with active regions larger than a few tens of Å.[20] With band bending taken into account, we typically need to compute transmission coefficients for structures considerably wider than 1000 Å, which cannot be treated with the standard transfer matrix method. There are several numerically stable, though computationally more onerous, methods for calculating transmission coefficients.[21–24] Recently, Frensley[23] pointed out that by following the approach taken by Lent and Kirkner[24] in solving the 2D effective-mass Schrödinger equation with finite element techniques, and formulating the heterostructure tunneling problem as a system of sparse linear equations, numerical stability can be achieved. For our calculation of hole transmission coefficients, we have generalized this method to multiband tight-binding models; the details will be described elsewhere.[25]

III. RESULTS AND DISCUSSION

In general, two-terminal interband tunnel devices can be classified according to their terminal types: (1) two *n*-type electrodes; (2) two *p*-type electrodes; and (3) one *n*- and one *p*-type electrode. The three categories are schematically illustrated in Fig. 2 by, respectively, (a) the InAs–GaSb–InAs structure, (b) the GaSb–InAs–GaSb structure, and (c) the InAs–GaSb–AlSb–GaSb structure. As shown in Fig. 2, the conduction band of InAs overlaps in energy with the valence bands of GaSb, leading to the possibility of interband transport. We choose the InAs conduction band edge as the origin of the energy scale, placing the GaSb valence band edge at 0.154 eV. Below we present results for each of the three device structures depicted in Fig. 2, with emphasis on transport in the broken-gap energy range between the InAs conduction band edge and the GaSb valence band edge (0 to 0.154 eV).

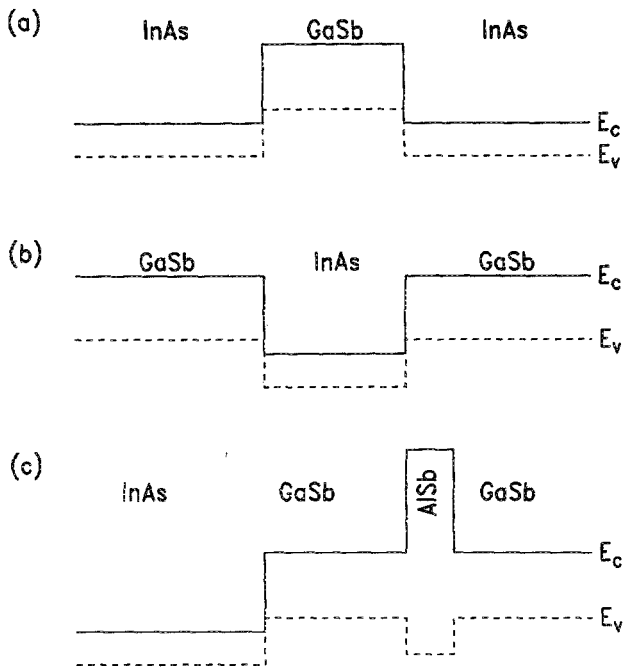

FIG. 2. Schematic energy band diagrams for (a) the InAs–GaSb–InAs interband tunnel structure, (b) the GaSb–InAs–GaSb structure, and (c) the InAs–GaSb–AlSb–GaSb structure.

A. InAs–GaSb–InAs

Figure 2(a) shows a schematic energy band diagram for the InAs–GaSb–InAs structure. In contrast to a double barrier heterostructure, in which resonant tunneling occurs via quasibound states localized by the barriers, quasibound hole states in the InAs–GaSb–InAs structure are formed in the GaSb layer due to the imperfect matching of InAs conduction-band and GaSb valence-band wave functions at the two InAs/GaSb interfaces. Consequently, resonant transport in this device can occur despite the absence of classically forbidden barrier regions. We refer to this as resonant transport rather than resonant tunneling since no classically forbidden regions are involved.

In Fig. 3 we show the transmission coefficients over the broken-gap energy range for an InAs–GaSb–InAs structure at several different values of $\mathbf{k}_{\parallel}$ ($\mathbf{k}_{\parallel}$ being the component of the wave vector parallel to the heterostructure interfaces, given in units of $2\pi/a$ throughout this paper). In addition to the calculations using the eight-band effective bond orbital model (shown as solid lines), we have shown, for comparison, the results obtained with a simple two-band model in which only the lowest conduction band and the light-hole band are included (dotted lines). At $\mathbf{k}_{\parallel}=0$, the two- and eight-band results are qualitatively similar, yielding a single light-hole transmission resonance peak which we designate as LH1. Since the formation of the quasibound state does not involve any barriers, the transmission resonance width is rather large, $-\Delta E\approx 30$ meV, corresponding to an intrinsic quasibound state lifetime of ~ 20 fs.

For $\mathbf{k}_{\parallel}\neq 0$, transmission coefficients calculated using the eight-band model exhibit a set of heavy-hole resonances not present in the two-band calculation. The heavy-hole reson-

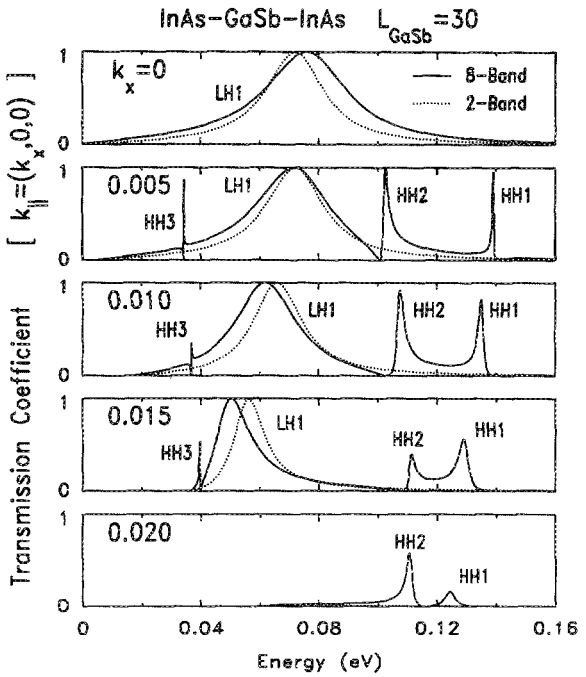

FIG. 3. Transmission coefficients for the InAs–GaSb–InAs structure calculated for a series of $k_{||}$ values using the effective bond-orbital model (solid lines), and using a simple two-band model (dotted lines). The width of the GaSb quantum well is 30 monolayers, and k_x values labeling the plots are given in units of $2\pi/a$.

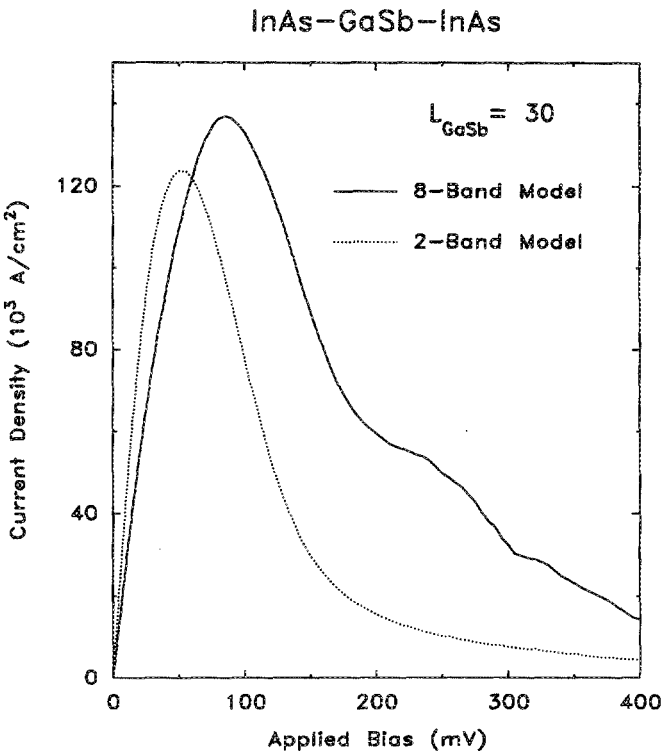

FIG. 4. Current–voltage characteristics for the InAs–GaSb–InAs structure calculated using the effective bond-orbital model (solid lines), and using a simple two-band model (dotted lines). The width of the GaSb quantum well is 30 monolayers.

ances are considerably narrower than the light-hole resonance, indicating that the coupling between GaSb heavy-hole states and InAs conduction-band states is much weaker than the GaSb light hole–InAs conduction-band coupling. The LH1 resonance is in general well approximated by the two-band model, although the eight-band model LH1 peak position decreases in energy more rapidly with increasing $k_{||}$. The nonparabolic dispersion in the GaSb quantum well band structure caused by heavy hole–light hole mixing is also evident in the position of the HH2 peaks as a function of k_x.

In Fig. 4 we show calculated current–voltage characteristics for the InAs–GaSb–InAs structure. Results from both the eight-and two-band calculations are shown. The eight-band result predicts somewhat higher peak current density and peak voltage, and exhibits a shoulder at 150 mV above the peak. We attribute this shoulder to the heavy-hole resonances. Our present calculation includes only elastic tunneling currents; in an actual device where inelastic scattering processes also contribute to the current, the heavy-hole shoulder would be part of the valley current.

B. GaSb–InAs–GaSb

Figure 2(b) shows the GaSb–InAs–GaSb structure. This device operates on the same principle as the InAs–GaSb–InAs device, relying on the barrier-less resonant interband transport mechanism, with holes transported between the GaSb electrodes via the InAs conduction band states. It may be regarded, in fact, as the p-type version of the InAs–GaSb–InAs device. Figure 5 shows the transmission coefficient for

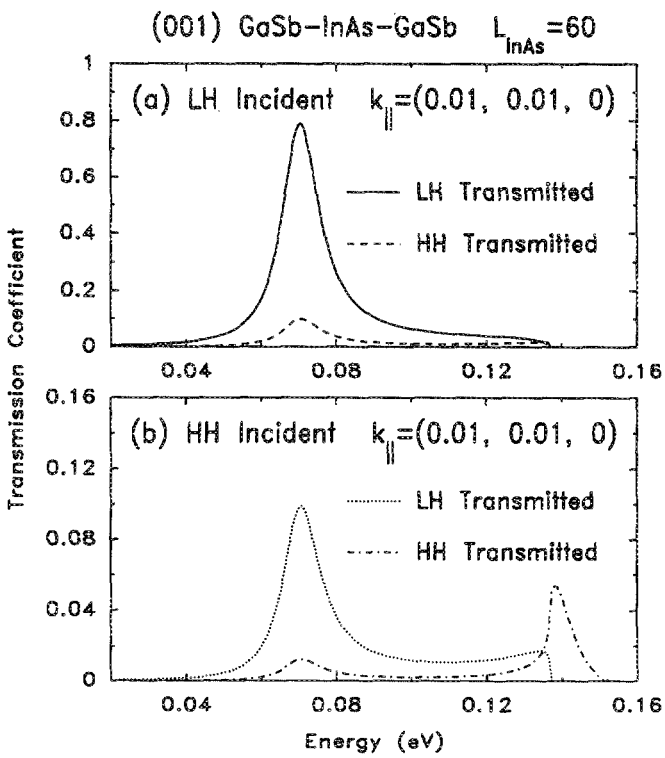

FIG. 5. Transmission coefficients calculated for the GaSb–InAs–GaSb structure for (a) an incident GaSb light-hole state and (b) an incident GaSb heavy-hole state. The width of the InAs quantum well is 60 monolayers, and $k_{||}$ = (0.01,0.01,0). Note that different vertical scales are used in (a) and (b).

a GaSb–InAs–GaSb structure in the broken-gap energy range for states with $\mathbf{k}_{\parallel} = (0.01,0.01,0)$. Since both the incident and the transmitted waves can contain either light-hole or heavy-hole states, the transmission coefficient has four components. We denote the four components by LH-CB-LH, LH-CB-HH, HH-CB-LH, and HH-CB-HH. In all four components we observe the CB1 resonance corresponding to the lowest quasibound states in the InAs layer. The LH-CB-LH component provides the dominant contribution to the total transmission coefficient due to the strong coupling between the GaSb light-hole band and the InAs conduction band. The LH-CB-HH and the HH-CB-LH components each contribute equally to the transmission coefficient, totaling almost 20%. The HH-CB-HH component is quite small, although it shows the CB2 resonance not seen in the other components due to the fact that the CB2 resonance lies above the available GaSb light hole states at this $\mathbf{k}_{\parallel}$ value.

C. InAs–GaSb–AlSb–GaSb

In the final example we examine an interband device which has one *n*-type electrode and one *p*-type electrode. The most basic device of this type consists simply of an interface between *n*-type InAs and *p*-type GaSb,[8] which can be thought of as a heterojunction Esaki diode. Substantial improvement in the performance of this device can be obtained by inserting a thin AlSb barrier layer on the GaSb side of the interface, as depicted in Fig. 2(c), forming a GaSb quantum well and thereby inducing resonances for achieving enhanced tunneling.[10] In Fig. 6 we show the transmission coefficients for the InAs–GaSb–AlSb–GaSb device calculated for $\mathbf{k}_{\parallel}$ values of (0,0,0), (0.0075, 0, 0), and (0.015, 0, 0) using both the two-band model (dotted lines) and the eight-band model (solid lines for transmitted LH states and dashed lines for transmitted HH states). The widths of the GaSb quantum well and the AlSb barrier are 75 and 9 Å, respectively. At $\mathbf{k}_{\parallel} = 0$, the light-hole transmitted component shows a single resonance peak identified as LH1, and there is no heavy-hole transmitted component. In this case the two-band model result approximates the eight-band result reasonably well. For $\mathbf{k}_{\parallel} \neq 0$, a small but nonnegligible heavy-hole transmitted component is found in addition to the light-hole transmitted component which still provides the dominant contribution. For $\mathbf{k}_{\parallel} = (0.0075, 0, 0)$, two wide peaks and a single narrow peak are found. By studying the wave functions of the transmitting states, the narrow peak is identified as the HH1 resonance, while the two wide peaks are found to be resonances corresponding to LH1-HH2 mixed states. Because of the strong hole-mixing effects, the calculation for this structure using the two-band model compares very unfavorably to the more realistic eight-band model calculation. An additional feature in the InAs–GaSb–AlSb–GaSb structure is the lack of inversion symmetry. As a result, splitting of degenerate energy levels is expected.[26] This can be seen at $\mathbf{k}_{\parallel} = (0.015, 0, 0)$, where the larger dispersion makes the splitting clearly observable for the two higher peak structures. Note that no such splitting is seen for the more symmetric InAs–GaSb–InAs structure at comparable $\mathbf{k}_{\parallel}$ values (see Fig. 3).

Figure 7 shows the current–voltage characteristics for an

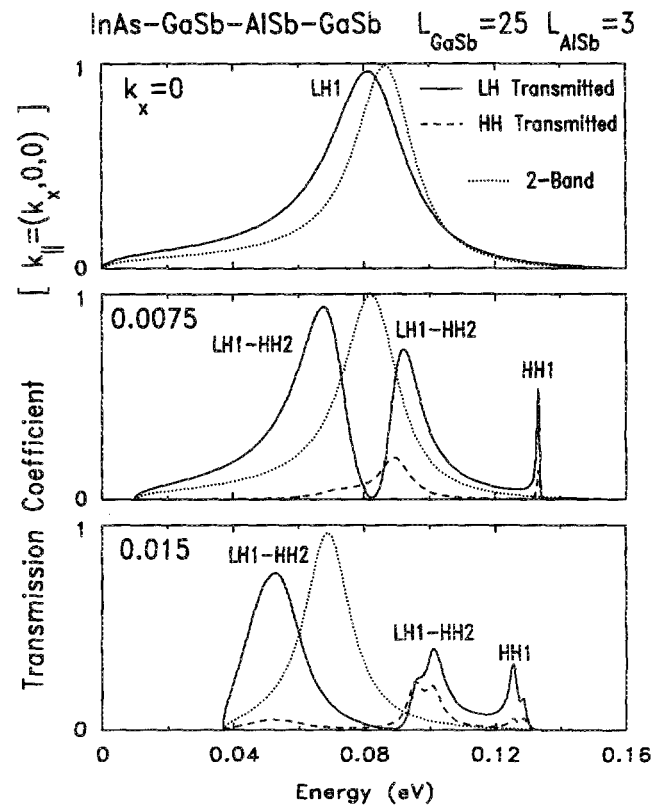

FIG. 6. InAs–GaSb–AlSb–GaSb transmission coefficients for a series of $\mathbf{k}_{\parallel}$ values. The width of the GaSb quantum well is 25 monolayers, and the width of the AlSb layer is 3 monolayers. Both the two-band model results (dotted lines) and the eight-band model results (solid lines for LH transmitted, dashed lines for HH transmitted) are shown.

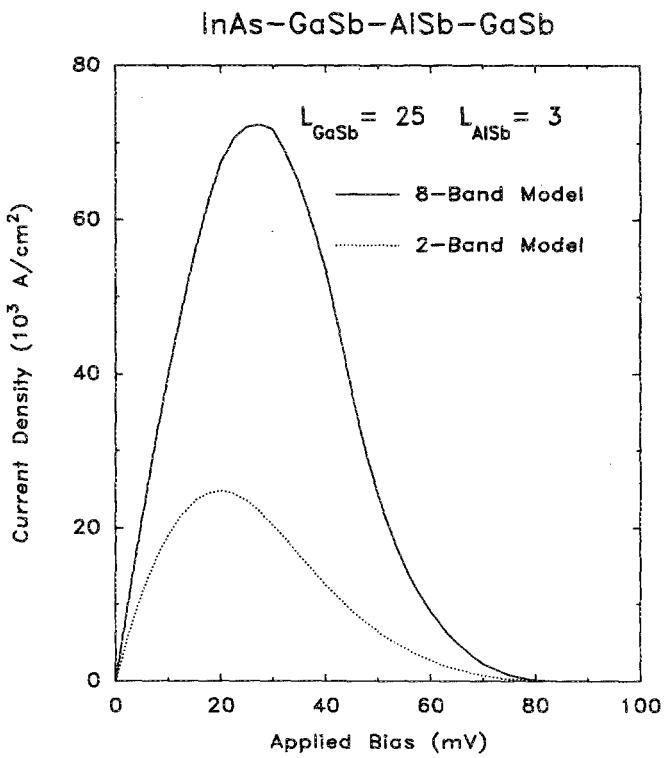

FIG. 7. Current–voltage characteristics for the InAs–GaSb–AlSb–GaSb structure calculated using the effective bond-orbital model (solid lines), and using a simple two-band model (dotted lines).

InAs–GaSb–AlSb–GaSb structure calculated using the two- and the eight-band models. The peak current density in the eight-band J–V curve is more than three times higher than the two-band peak. At first it may be tempting to attribute this large discrepancy to additional currents due to heavy-hole resonances. A more careful analysis shows that this is false. In a diode with InAs and GaSb terminals, a transmission resonance contributes to the elastic tunneling current only if it lines up with both the InAs electron Fermi sea and GaSb hole Fermi sea in the two electrodes. As a result of this rather stringent requirement, the amount of elastic tunneling current in this type of device is very sensitive to the positions of the resonance peaks. As seen in Fig. 6, the nature of the LH1 resonance is drastically altered due to band mixing effects, splitting into two LH1-HH2 peaks. The difference in the hole transmission spectra accounts for the large discrepancy in the peaks current density computed with the two different models.

A broader view of the influence of heavy-hole states on J–V characteristics of InAs–GaSb–AlSb–GaSb tunnel structures is shown in Fig. 8, where we plot the two-band and the eight-band theoretical peak current densities as functions of GaSb well width. Due to the inclusion of heavy-hole states, the eight-band result contains considerably more structure. For narrow GaSb wells, the two-band model predicts no resonance in the broken-gap energy range, while the eight-band model shows the HH1 resonance. This is responsible for the higher peak current densities predicted by the eight-band model for narrow GaSb wells. For wider wells, the two-band model predicts a single wide light-hole resonance, while the eight-band model shows the split pair of LH1-HH2 wide resonances, as seen in Fig. 6. We see that while the overall magnitudes of the peak current densities predicted by the two models are similar, the eight-band model shows two local maxima rather than the one predicted by the two-band model.

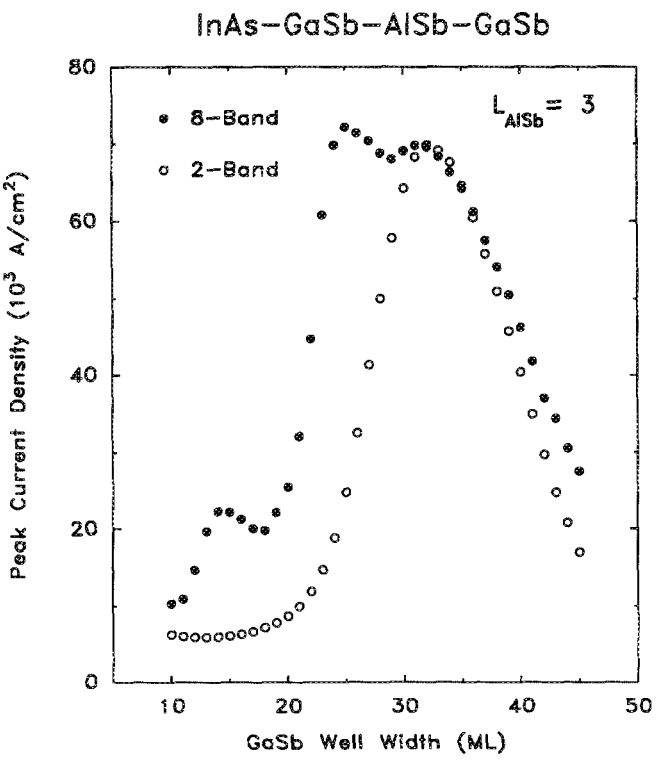

FIG. 8. Dependence of theoretical peak current densities on GaSb well width for the InAs–GaSb–AlSb–GaSb tunnel structure, calculated using the effective bond-orbital model (filled circles), and using a two-band model (open circles). The width of the AlSb barrier is three monolayers.

IV. SUMMARY

InAs/GaSb/AlSb-based interband device structures have been studied using a newly developed method for computing heterostructure transmission coefficients. We have implemented this method for the effective bond-orbital model, which realistically describes the relevant band structure near the Brillouin zone center. Comparing our calculations with results obtained using a simple two-band model which includes only the lowest conduction band and the light-hole band, we find that the presence of heavy-hole states gives rise to additional heavy-hole resonances and introduces substantial band mixing effects in device structures containing GaSb quantum wells. We have calculated current–voltage characteristics for the InAs–GaSb–InAs and InAs–GaSb–AlSb–GaSb devices using both models, and have shown that the influence of the heavy-hole states could be substantial.

ACKNOWLEDGMENTS

The authors would like to thank W. R. Frensley, C. S. Lent, Y. C. Chang, and J. N. Schulman for helpful discussions. One of us (E. T. Y.) would like to acknowledge financial support from the AT&T Foundation. This work is supported by the Office of Naval Research (ONR) under Grant No. N00014-89-J-1141.

[1] G. J. Gaultieri, G. P. Schwartz, R. G. Nuzzo, R. J. Malik, and J. F. Walker, J. Appl. Phys. **61**, 5337 (1987).
[2] G. J. Gaultieri, G. P. Schwartz, R. G. Nuzzo, and W. A. Sunder, J. Appl. Phys. **49**, 1037 (1986).
[3] We assume transitivity to obtain the InAs/AlSb band offset value.
[4] J. R. Söderström, D. H. Chow, and T. C. McGill, Appl. Phys. Lett. **55**, 1094 (1989).
[5] L. F. Luo, R. Beresford, and W. I. Wang, Appl. Phys. Lett. **55**, 2023 (1989).
[6] R. Beresford, L. F. Luo, and W. I. Wang, Appl. Phys. Lett. **56**, 551, 952 (1990).
[7] K. Taira, I. Hase, and K. Kawai, Electron. Lett. **25**, 1708 (1989).
[8] D. A. Collins, E. T. Yu, Y. Rajakarunanayake, J. R. Söderström, D. H. Chow, D. Z.-Y. Ting, and T. C. McGill, Appl. Phys. Lett. **57**, 683 (1990).
[9] L. Yang, J. F. Chen, and A. Y. Cho, J. Appl. Phys. **68**, 2997 (1990).
[10] D. Z.-Y. Ting, D. A. Collins, E. T. Yu, D. H. Chow, and T. C. McGill, Appl. Phys. Lett. **57**, 1257 (1990).
[11] D. A. Collins and T. C. McGill, 1990 IEEE Intl. Electron Devices Meeting Technical Digest, 1990, Vol. 945.
[12] J. R. Söderström, E. T. Yu, M. K. Jackson, Y. Rajakarunanayake, and T. C. McGill, J. Appl. Phys. **68**, 1372 (1990).
[13] D. Z.-Y. Ting, E. T. Yu, D. A. Collins, D. H. Chow, and T. C. McGill, J. Vac. Sci. Technol. B **8**, 810 (1990).
[14] E. T. Yu, D. A. Collins, D. Z.-Y. Ting, D. H. Chow, and T. C. McGill, Appl. Phys. Lett. **57**, 2675 (1990).
[15] C. B. Duke, *Tunneling in Solids*, Solid State Physics, Suppl. 10 (Academic, New York, 1969).
[16] Y. C. Chang, Phys. Rev. B **37**, 8215 (1988).
[17] E. O. Kane, in *Semiconductors and Semimetals*, edited by R. K. Willard-

and A. C. Beer (Academic, New York, 1966), Vol. 1, p. 75.
[18] E. O. Kane, in *Tunneling Phenomena in Solids*, edited by E. Burstein and S. Lundqvist (Plenum, New York, 1969), p. 1.
[19] See, for example, J. N. Schulman and Y. C. Chang, Phys. Rev. B **27**, 2346 (1983).
[20] C. Mailhiot and D. L. Smith, Phys. Rev. B **33**, 8360 (1986).
[21] G. Wachutka, Phys. Rev. B **34**, 8512 (1986).
[22] D. Y. K. Ko and J. C. Inkson, Phys. Rev. B **38**, 9945 (1988).
[23] W. R. Frensley (private communication).
[24] C. S. Lent and D. J. Kirkner, J. Appl. Phys. **67**, 6353 (1990).
[25] D. Z.-Y. Ting, E. T. Yu, and T. C. McGill (unpublished).
[26] See, for example, P. T. Landsberg, in *Solid State Theory; Methods and Applications*, edited by P. T. Landsberg (Wiley-Interscience, London, 1969), p. 506.